The first amino acid bound manganese–calcium clusters: a {[MnIII3Ca]2} methylalanine complex, and a [MnIII6Ca] trigonal prism

Dalton Transactions

ROYAL SOCIETY OF CHEMISTRY

COMMUNICATION

View Article Online
View Journal

Cite this: DOI: 10.1039/d0dt01916j

Received 28th May 2020,
Accepted 17th July 2020

DOI: 10.1039/d0dt01916j

rsc.li/dalton

The first amino acid bound manganese–calcium clusters: a {[$Mn^{III}_3Ca]_2$} methylalanine complex, and a [Mn^{III}_6Ca] trigonal prism†

Thomais G. Tziotzi,[a] Evangelos K. Andreou,[a] Eirini Tzanetou,[a] Dimitris A. Kalofolias,[a] Daniel J. Cutler,[b] Marek Weselski,[c] Milosz Siczek,[c] Tadeusz Lis,[c] Euan K. Brechin[b] and Constantinos J. Milios*[a]

An amino acid containing octanuclear heterometallic {[$Mn^{III}_3Ca]_2$} cluster has been synthesized, alongside a structurally-related trigonal prismatic [$Mn^{III}_6Ca]^{2+}$ cage.

Perhaps one of the most stimulating events in the course of bioinorganic chemistry was the discovery of a pentanuclear heterometallic manganese–calcium cluster in the active center of Photosystem II (PSII). The Oxygen Evolving Center (OEC) of PSII is responsible for the photosynthetic process, more specifically for the oxidative splitting of water to molecular dioxygen, four protons and 4 electrons (per two water molecules), by sunlight. Molecular oxygen is consequently released into the atmosphere, while the protons produced are used to generate ATP chemical energy coins.[1] Yet, the complete nature and chemical composition of PSII has been puzzling bioinorganic chemists and crystallographers for several years, with details at the atomic level only appearing in the last two decades.[2] The water splitting site is positioned at the heart of the OEC and consists of a pentanuclear [Mn_4Ca] complex, whose structure has been described as a cubane-like $[Mn_3CaO_4]^{n+}$ moiety linked to a fourth Mn^{n+} atom *via* oxo-bridges. The structure is held in position by the carboxylate groups of the side chains of amino acids (D1-Asp170, D1-Glu333, D1-Asp342, CP43-Glu354), as well as the carboxy-terminal residue of D1-Ala344, responsible for the intra-cubane linkage of the calcium ion to a manganese ion. The role of the pentametallic cluster is to serve as an e^- donor during consequent cycles through a procedure that involves four oxidation steps, S_{0-4} (Kok cycle). At the end of the catalytic cycle the cluster, short of 4 e^-, "engages" two water molecules oxidizing them to O_2, protons and e^-, in order to regenerate.[3] During the last years numerous compounds have been synthesized and characterized as potential synthetic models of the active center of the enzyme. More specifically, compounds have been reported displaying structural, spectroscopic, and/or catalytic similarity to the OEC. Most of these compounds are polynuclear manganese clusters with the metal ions in various oxidation states.[4] However, only a few examples of mixed metal manganese–calcium clusters (*i.e.* those containing both of the metal centers present in the active site) displaying structural similarities and/or similar metal-content to the OEC have been reported.[5]

We previously reported the first examples of polynuclear manganese clusters containing amino acid ligands, in which the manganese ions existed in moderate-high oxidation states.[6] This motivated us to investigate whether amino acids could also be used to build heterometallic Mn/Ca clusters, and herein report the synthesis, structure and magnetic properties of the first two clusters of this new family, namely {[Mn^{III}_3CaO(OH)(mAla)$(O_2CPh)_3(HL^a)_2$(MeOH)]$_2$}·6.2MeCN·0.9H_2O (**1**·6.2MeCN·0.9H_2O) and [$Mn^{III}_6CaO_3L^b_6(H_2O)_3$]$(ClO_4)_2$·14.1$H_2O$ (**2**·14.1H_2O), using the amino acid methylalanine, mAlaH, and either the naphthalene-based triol ligand 2-(β-naphthalideneamino)-2-hydroxyethyl-1-propanol, H_3L^a, or the Schiff-base ligand created *in situ* upon the condensation of mAlaH and salicylaldehyde, H_2L^b, as co-ligands (Scheme S1†). To the best of our knowledge compounds **1** and **2** are the first examples of any heterometallic Mn/Ca clusters containing amino acids as ligands, with obvious relation to OEC, mimicking not only the metallic content of the active center, but also the amino acid moiety bridging the Mn and Ca ions.

$Mn(ClO_4)_2$·6H_2O (181 mg, 0.5 mmol), $Ca(O_2CPh)_2$·2H_2O (318 mg, 1 mmol), mAlaH (51 mg, 0.5 mmol) and H_3L^a (130 mg, 0.5 mmol) were stirred in MeCN/MeOH (1 : 1, 20 ml) in the presence of excess base, NEt_3, for 2 hours to form a dark brown suspension. The precipitate was removed by filtration and the dark-brown solution was layered with Et_2O (20 ml) to form dark brown crystals of {[Mn^{III}_3CaO(OH)(mAla)$(O_2CPh)_3$

[a]Department of Chemistry, The University of Crete, Voutes, 71003 Herakleion, Greece. E-mail: komil@uoc.gr
[b]EaStCHEM School of Chemistry, The University of Edinburgh, David Brewster Road, Edinburgh, EH9 3FJ, UK
[c]Faculty of Chemistry, University of Wroclaw, 50-283 Wroclaw, Poland

†Electronic supplementary information (ESI) available. CCDC 1816563 and 1999601. For ESI and crystallographic data in CIF or other electronic format see DOI: 10.1039/d0dt01916j

$(HL^a)_2(MeOH)]_2\}\cdot 6.2MeCN\cdot 0.9H_2O$ (**1**· 6.2MeCN·0.9H_2O) after 4 days in ~30% yield. For **2**, $Mn(ClO_4)_2\cdot 6H_2O$ (181 mg, 0.5 mmol), $Ca(NO_3)_2\cdot 4H_2O$ (354 mg, 1.5 mmol), mAlaH (25 mg, 0.5 mmol), salicylaldehyde (0.0552 mL, 0.5 mmol) and NBu_4MnO_4 (MeCN solution, 0.05 M, 1 ml, 0.05 mmol) were stirred in MeCN (20 ml) in the presence of excess base NEt_3, for 30 minutes to form a dark brown solution, which was left to slowly evaporate, forming dark brown crystals of $[Mn^{III}_6CaO_3L^b_6(H_2O)_3](ClO_4)_2\cdot 14.1H_2O$ (**2**·14.1H_2O) after ~2 days, in ~40% yield‡.

Compound **1** crystallizes in the triclinic space group $P\bar{1}$, with the asymmetric unit (ASU) comprising half the molecule. Its structure (Fig. 1) consists of two $\{Mn^{III}_3Ca^{II}\mu_4\text{-}O\}$ tetrahedra linked together *via* two μ_3-OH ions (O1 and symmetry equivalent (s.e.)), which also bridge to Mn1 and s.e. The basal plane of the tetrahedron comprises an oxo-centered $[Mn^{III}_3O]^{7+}$ triangle in which the O^{2-} ion (O2 and s.e.) resides 0.233 Å 'above' the $[Mn^{III}_3]$ plane, towards the center of the cage, bonding to the Ca^{2+} ion at a distance of ~2.63 Å. The benzoate ligands are of three types: one μ- bridges between Ca1 and Mn1′ (and s.e.), linking the two halves of the molecule; one μ- bridges between Mn2 and Mn3 (and s.e.) in the basal plane of the tetrahedron; and one is terminally bonded to Mn1 (and s.e.), the non-bonded arm H-bonding to the protonated arm of the neighbouring triol ligand (O2C···(H)–O15F, 2.67 Å). Each $\eta^2{:}\eta^1{:}\mu\text{-}HL^{a\ 2-}$ ligand connects a Mn^{III} ion in the basal plane of the tetrahedron to the Ca^{II} ion in the upper vertex, with the chelating mAla ligand being bound to Mn1 (and s.e.) forming a five-membered ring through the N and one $O_{carboxylate}$ atoms. The manganese ions are all in the 3+ oxidation state (BVS = 3.04, 2.94 and 2.89, for Mn1, Mn2 and Mn3, respectively) displaying Jahn–Teller elongated octahedral geometries (O1C–Mn1–O2A, 2.170–2.210 Å; O1B–Mn2–O1C, 2.138–2.498 Å; O2B–Mn3–O2A, 2.142–2.509 Å). The *JT* axes all lie within the $[Mn^{III}_3]$ plane. The Ca^{II} ions are seven-coordinate adopting capped octahedral geometries (SHAPE analysis[7]), the last coordination site being occupied by a MeOH molecule. The Mn···Mn distances fall in the range ~3.2–3.4 Å, while the Mn···$Ca_{tetrahedron}$ distance are in the narrow range ~3.4–3.5 Å. Intermolecular interactions are mediated *via* the π–π stacking of the naphthyl groups of the HL^{2-} and benzoate ligands (C···C, ~3.4 Å).

Compound **2** crystallizes in the trigonal space group $R\bar{3}c$ (with two crystallographically independent cluster cations). Their metallic skeleton consists of a $\{Mn^{III}_6\}$ trigonal prism encapsulating a nine-coordinate Ca^{II} ion at its center (Fig. 2). Each triangular face describes an almost ideal equilateral triangle ($Mn^{III}\cdots Mn^{III}$ ~ 5.26–5.28 Å), the Mn ions being bridged by one *syn*, *anti* carboxylate group of a mAla Schiff-base ligand (O23, O24, O33 and O34 and s.e.), which further bridges to the central divalent calcium ion in a $\eta^2{:}\eta^1{:}\eta^1{:}\mu_3$-fashion. The two triangles are interconnected by three $\mu\text{-}H_2O$ molecules (Mn–O_W–Mn, 81.85°) and three $\mu_3\text{-}O^{-2}$ ligands (O2 and s.e, Mn–O2–Mn, 114.28°) which also bind to the central Ca^{II} center. The approximate dimensions of the cage are 5.3 (Mn–Mn, triangular face) × 3.1 Å (Mn–Mn, upper-to-lower vertex), with the Mn–Ca distance being approximately 3.4 Å. The overall 2+ charge of the complex cation is compensated by the presence of perchlorate anions. The manganese centers are six-coordinate and in the +3 oxidation state (BVS = 2.93), adopting *JT*-elongated geometries, the *JT* axes being oriented along the O_W–Mn–O(carboxylate) vectors, aligned midway between parallel and perpendicular to the $[Mn_3]$ plane. The central calcium ion is nine-coordinate with a tricapped trigonal prismatic $\{CaO_9\}$ geometry (SHAPE analysis[7]) with Ca–O distances in the range 2.446–2.511 Å. In the extended structure the clusters are surrounded by a large number of H_2O molecules, several of

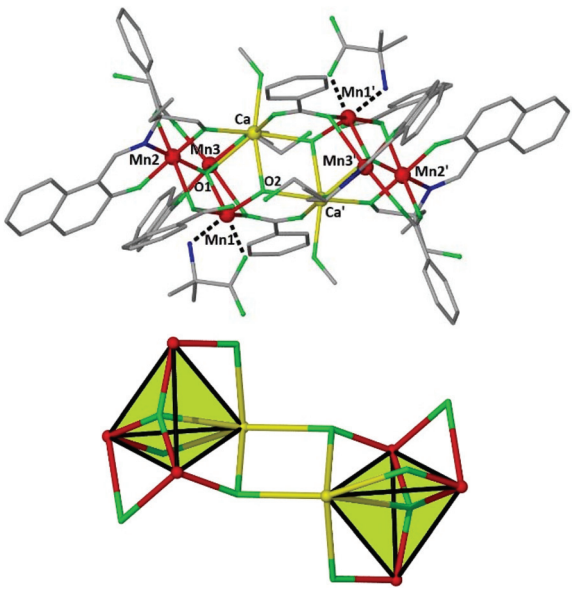

Fig. 1 The molecular structure of **1**, highlighting the chelate mode of the mAla ligands (top). The metallic core of **1**, showing the connection of the two $\{Mn_3CaO\}$ tetrahedral units (bottom). Color code: Mn^{III} = red, Ca^{II} = yellow, O = green, N = blue, C = grey. H-atoms and solvate molecules have been omitted for clarity.

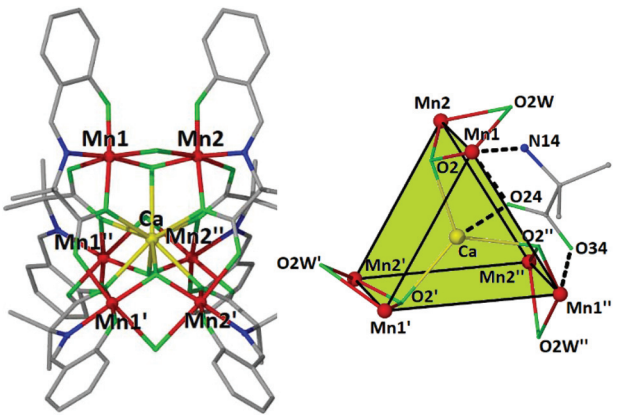

Fig. 2 The molecular structure of the dication of **2** (left). The metallic core of **2**, highlighting the coordination mode of the amino acid part of the Schiff-base, the bridging water molecules and the bridging $\mu_3\text{-}O^{2-}$ anions (right). Color code: Mn^{III} = red, Ca^{II} = yellow, O = green, N = blue, C = grey. H-atoms, counter ions and solvate molecules have been omitted for clarity.

which have partial occupancy, as well as several perchlorate anions. The solvate and coordinated μ-H_2O molecules, along with the perchlorate anions participate in a large number of hydrogen bonding interactions. There is also a significant number of C–H···O (from H_2O or ClO_4^- anions) interactions in the lattice that bridge the clusters together, creating a complicated 3D H-bonded framework (Fig. S1†). There are not any π–π or C–H···π interactions present.

The structural similarities of **1** and **2** to the actual OEC are: (i) the bridging mode of the carboxylate group of the amino acid ligand (D1-Ala344 in the OEC *vs.* mAla in **2** which bridges the Ca and Mn centers, (ii) the formation of a [Mn_3Ca] tetrahedron, (iii) the presence of the sp^2 N-atom of the mAla Schiff-base ligand in **2** mimicking the amide N-atoms present in the OEC, and (iv) the presence of six-coordinate Mn ions in all cases. In addition, the +3 oxidation state for all manganese centers may correspond to the dark stable S_1 state as has been suggested previously,[8] although it is still not clear whether S_1 adopts a [Mn_4^{III}] or a [$Mn_2^{IV}Mn_2^{III}$] state. Furthermore, the presence of the six bridging water molecules in **2** is of great biological importance, given the presence of the water molecules near the active site of the enzyme that serve as a substrate.

Variable temperature dc magnetic susceptibility data were collected for **1** and **2** in the temperature range 5.0–300 K under an applied field of 0.1 T, and are plotted as $\chi_M T$ *versus* T in Fig. 3 and 4. For **1**, the room temperature value of 8.35 cm^3 mol^{-1} K per {Mn_3Ca} unit is slightly lower than the theoretical value of 9.00 cm^3 mol^{-1} K expected for three non-interacting Mn^{III} centers (g = 2.00). Upon cooling $\chi_M T$ decreases slowly to ~7.49 cm^3 mol^{-1} K at ~130 K, before rapidly decreasing to a minimum value of 3.21 cm^3 mol^{-1} K at 5 K. This suggests the presence of weak antiferromagnetic exchange between the three Mn^{III} ions. For **2**, the room temperature $\chi_M T$ value of 17.63 cm^3 mol^{-1} K is very close to the theoretical value of 18.00 cm^3 mol^{-1} K expected for six non-interacting Mn^{III} centers (g = 2.00). Upon cooling $\chi_M T$ remains approximately constant until ~150 K, below which it increases slowly to reach ~19.32 cm^3 mol^{-1} K at ~35 K, before rapidly decreasing to a minimum value of 5.92 cm^3 mol^{-1} K at 5 K. This behavior is indicative of the presence of both ferro- and antiferromagnetic exchange interactions.

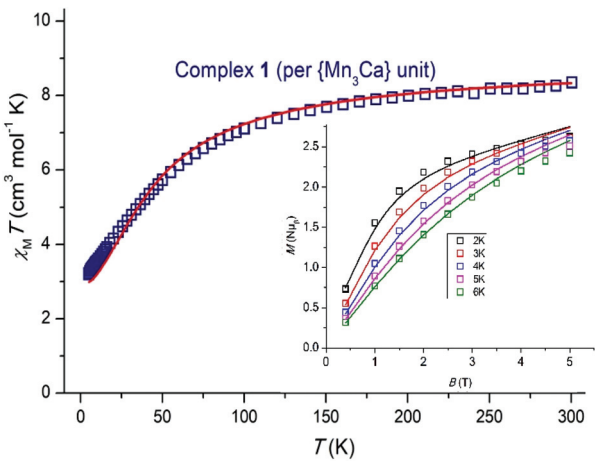

Fig. 3 $\chi_M T$ *vs.* T plot for complex **1** under an applied dc field of 1000 G. The solid lines represent fit of the data in the 5–300 K (see text for details). Inset: plot of reduced magnetization ($M/N\mu_B$) *versus* B for **1** in the field and temperature ranges 0–5 T and 2–6 K. The solid lines correspond to the fit of the data.

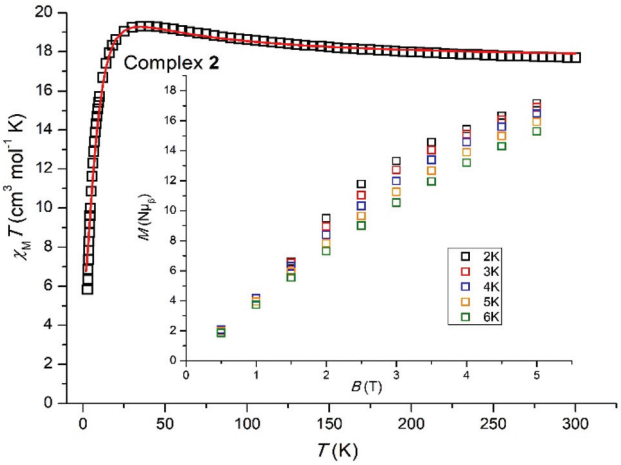

Fig. 4 $\chi_M T$ *vs.* T plot for complex **2** under an applied dc field of 1000 G. The solid lines represent fit of the data in the 5–300 K (see text for details). Inset: plot of reduced magnetization ($M/N\mu_B$) *versus* B for **2** in the field and temperature ranges 0–5 T and 2–6 K.

The susceptibility and magnetization data for **1** can be simultaneously fitted through the use of the program PHI[9] employing spin-Hamiltonian (1) and the exchange coupling scheme shown in Fig. S2,† where $\hat{S}$ is a spin-operator, J the pairwise exchange coupling constant, B the applied magnetic field, and D the axial zero field splitting parameter for the Mn^{III} ion. The exchange coupling model assumes one exchange interaction (J_1) between Mn1–Mn2 and Mn1–Mn3 mediated by one μ$_4$-O^{2-} bridge and one monoatomic-bridge benzoate ligand, and a second exchange interaction (J_2) between Mn2–Mn3 mediated by a μ$_4$-O^{2-} bridge and a bridging η^1:η^1:μ_2 benzoate. The best fit (Fig. 3) parameters are J_1 = +0.50 cm^{-1}, J_2 = −7.00 cm^{-1} and D_{Mn} = −6.56 cm^{-1} with g fixed, g_{Mn} = 1.98. The fit can be improved with the inclusion of an intermolecular exchange interaction term, zJ' = 0.12 cm^{-1}. A fit of the susceptibility data on its own using only the isotropic exchange part of spin-Hamiltonian (1) affords J_1 = +0.65 cm^{-1}, J_2 = −6.0 cm^{-1} with g_{Mn} = 1.98. These J values belong to a well-defined minimum for this system in the {0.0, +1.0 cm^{-1}}(J_1)–{−5.5, −7.5 cm^{-1}}(J_2) region, as shown by the contour error plot for the data of **1** as a function of J_1 and J_2 (Fig. S3†).

$$\hat{H} = -2J_1(\hat{S}_1 \cdot \hat{S}_2 + \hat{S}_1 \cdot \hat{S}_3) - 2J_2(\hat{S}_2 \cdot \hat{S}_3) - D(\hat{S}_{1z^2} + \hat{S}_{2z^2} + \hat{S}_{3z^2}) + g\mu_B\vec{B} \cdot \left(\sum_i \vec{\hat{s}}_i\right) \quad (1)$$

The weak ferromagnetic interaction J_1 may be potentially attributed to the small Mn–$O_{monoatomic\ benz}$–Mn angles present (Mn–O–Mn: 85.22 and 87.67°, for Mn1–Mn2 and Mn1–Mn3,

respectively), in addition to the *in-plane* arrangement of the *JT* axes with respect to the $\{Mn_2O_2\}$ plane.[10] In this simple "giant spin" model the ground-state of **1** is an $S = 2$ state, with the first $S = 3$ excited state located ~10 cm^{-1} above.

The size of complex **2** precludes the use of an anisotropic spin-Hamiltonian through standard computational techniques, but the susceptibility data can be fitted by adopting isotropic spin-Hamiltonian (2) which describes a 2-*J* model with: (1) J_1 between neighboring manganese centers located at the corners of the triangular faces, mediated by the *syn*, *anti* carboxylate group of the mAla Schiff-base ligand, and (ii) J_2 responsible for the connection of the two triangular faces, mediated by one μ-H_2O molecule and one μ_3-O^{2-} ligand (Fig. S4†).

$$\hat{H} = -2J_1(\hat{S}_1 \cdot \hat{S}_2 + \hat{S}_2 \cdot \hat{S}_3 + \hat{S}_1 \cdot \hat{S}_3 + \hat{S}_4 \cdot \hat{S}_5 + \hat{S}_5 \cdot \hat{S}_6 + \hat{S}_4 \cdot \hat{S}_6) - 2J_2(\hat{S}_1 \cdot \hat{S}_4 + \hat{S}_2 \cdot \hat{S}_5 + \hat{S}_3 \cdot \hat{S}_6) \quad (2)$$

Best fit parameters (Fig. 4) are $J_1 = -0.35$ cm^{-1}, $J_2 = +1.94$ cm^{-1} with g fixed, $g_{Mn} = 1.98$. This suggests the ground-state is a diamagnetic $S = 0$ state with the first $S = 1$ excited state located only ~0.35 cm^{-1} above. Magnetization data are in agreement with this picture (Fig. 4) with M rising in a near linear fashion with B.

Conclusions

In conclusion, we have reported the synthesis and characterization of the first two examples of heterometallic Mn/Ca clusters containing an amino acid ligand, methylalanine. Both species are structurally related to the heterometallic cluster found in the active site of the OEC of PSII. Magnetic susceptibility and magnetization measurements reveal the presence of weak antiferro- and ferromagnetic exchange interactions in agreement with magneto-structural correlations developed for structurally similar Mn^{III} clusters. Attempts are currently underway in order to probe the possibility of isolating heterometallic Mn/Ca species upon employment of the natural amino acids Asp, Glu and/or Ala, as a means of modelling the actual content of the OEC.

Conflicts of interest

There are no conflicts to declare.

Acknowledgements

The research work was supported by the Hellenic Foundation for Research and Innovation (HFRI) and the General Secretariat for Research and Technology (GSRT), under the HFRI PhD Fellowship grant (GA no. 4826). Part of this work was carried out in fulfillment of the requirements for the Master thesis of EKA according to the curriculum of the International Graduate Program in "Inorganic Biological Chemistry", which operates at the University of Ioannina within the collaboration of the Departments of Chemistry of the Universities of Ioannina, Athens, Thessaloniki, Patras, Crete, and the Department of Chemistry of the University of Cyprus. EKB thanks the EPSRC for funding grants EP/N01331X/1 and EP/P025986/1.

Notes and references

‡Crystal data for **1**·6.2MeCN·0.9H_2O: $C_{128.4}H_{144.4}Ca_2Mn_6N_{12.2}O_{34.9}$, $M = 2826.75$, triclinic, space group $P\bar{1}$, $a = 14.303(4)$ Å, $b = 15.673(5)$ Å, $c = 15.979(5)$ Å, $\alpha = 107.04(3)°$, $\beta = 99.23(3)°$, $\gamma = 97.21(3)°$, $V = 3323.5(19)$ $Å^3$, $Z = 1$, $T = 80$ K, R_1 ($I > 2\sigma$) = 0.067 and wR_2 (all data) = 0.201 for 29 522 reflections collected, 12 519 observed reflections ($I > 2\sigma(I)$) of 18 327 ($R_{int} = 0.039$) unique reflections, GOF = 1.01. Crystal data for **2**·14.1H_2O: $C_{66}H_{100.20}CaCl_2Mn_6N_6$ $O_{46.10}$, $M = 2155.94$, trigonal, space group $R\bar{3}c$, $a = 21.029(4)$ Å, $c = 143.48(6)$ Å, $V = 54\,949(31)$ $Å^3$, $Z = 24$, $T = 100$ K, R_1 ($I > 2\sigma$) = 0.106 and wR_2 (all data) = 0.208 for 40 308 reflections collected, 6462 observed reflections ($I > 2\sigma(I)$) of 11 186 ($R_{int} = 0.099$) unique reflections, GOF = 1.13. Full details can be found in the CIF files with CCDC reference numbers 1816563 and 1999601, for **1** and **2**, respectively.†

1 Representative references and refs therein: (*a*) J. Barber, *Chem. Soc. Rev.*, 2009, **38**, 185; (*b*) S. Mukhopadhyay, S. K. Mandal, S. Bhaduri and W. H. Armstrong, *Chem. Rev.*, 2004, **104**, 3981.

2 (*a*) A. Zouni, H.–T. Witt, J. Kern, P. Fromme, N. Krauss, W. Saenger and P. Orh, *Nature*, 2001, **409**, 739; (*b*) K. N. Ferreira, T. M. Iverson, K. Maghlaoui, J. Barber and S. Iwata, *Science*, 2004, **303**, 1831; (*c*) A. Guskov, J. Kern, A. Gabdulkhakov, M. Broser, A. Zouni and W. Saenger, *Nat. Struct. Mol. Biol.*, 2009, **16**, 334; (*d*) N. Kamiya and J. R. Shen, *Proc. Natl. Acad. Sci. U. S. A.*, 2003, **100**, 98; (*e*) Y. Umena, K. Kawakami, J.-R. Shen and N. Kamiya, *Nature*, 2011, **473**, 55.

3 B. Kok, B. Forbush and M. McGloin, *Photochem. Photobiol.*, 1970, **11**, 457.

4 See for example: (*a*) U. Bossek, H. Hummel, T. Weyhermüller, K. Wieghardt, S. Russell, L. Van der Wolf and U. Kolb, *Angew. Chem., Int. Ed. Engl.*, 1996, **35**, 1552; (*b*) J. B. Vincent, H. –R. Chang, K. Folting, J. C. Huffman, G. Christou and D. N. Hendrickson, *J. Am. Chem. Soc.*, 1987, **109**, 5703; (*c*) X. Li, D. P. Kessissoglou, M. L. Kirk, V. L. Pecoraro and C. J. Bender, *Inorg. Chem.*, 1988, **27**, 1; (*d*) V. Tangoulis, D. A. Malamatari, G. A. Spyroulias, C. P. Raptopoulou, A. Terzis and D. P. Kessisoglou, *Inorg. Chem.*, 2000, **39**, 2621; (*e*) J. B. Vincent, C. Christmas, H.-R. Chang, Q. Li, P. D. W. Boyd, J. C. Huffman, D. N. Hendrickson and G. Christou, *J. Am. Chem. Soc.*, 1989, **111**, 2086; (*f*) W. F. Ruettinger, C. Campana and G. C. Dismukes, *J. Am. Chem. Soc.*, 1997, **119**, 6670; (*g*) S. K. Chandra and A. Chakravorty, *Inorg. Chem.*, 1991, **30**, 3795; (*h*) E. C. Sanudo, V. A. Grillo, M. J. Knapp, J. C. Bollinger, J. C. Huffman, D. N. Hendrickson and G. Christou, *Inorg. Chem.*, 2002, **41**, 2441; (*i*) H. Chen, J. W. Faller, R.-H. Crabtree and G. W. Brudvig, *J. Am. Chem. Soc.*, 2004, **126**, 7345.

5 (*a*) A. Mishra, W. Wernsdorfer, K. A. Abboud and G. Christou, *Chem. Commun.*, 2005, 54; (*b*) I. J. Hewitt, J.-K. Tang, N. T. Mandhu, R. Clèrac, G. Buth, C. E. Anson and A. K. Powell, *Chem. Commun.*, 2006, 2650; (*c*) S. Nayak, H. P. Nayek, S. Dehnen, A. K. Powell and J. Reedijk, *Dalton Trans.*, 2011, **40**, 2699; (*d*) Y. J. Park, J. W. Ziller and A. S. Borovik, *J. Am. Chem. Soc.*, 2011, **133**, 9258; (*e*) V. Kotzabasaki, M. Siczek, T. Lis and C. J. Milios, *Inorg. Chem. Commun.*, 2011, **14**, 213; (*f*) J. S. Kanady, P.-H. Lin, K. M. Carsch, R. J. Nielsen, M. K. Takase, W. A. Goddard III and T. Agapie, *J. Am. Chem. Soc.*, 2014, **136**, 14373; (*g*) M. Kose, P. Goring, P. Lucas and P. Mckee, *Inorg. Chim. Acta*, 2015, **435**, 232; (*h*) J. S. Kanady, E. Y. Tsui, M. W. Day and T. Agapie, *Science*, 2011, **333**, 733; (*i*) E. S. Koumousi, S. Mukherjee, C. M. Beavers, S. J. Teat, G. Christou and T. C. Stamatatos, *Chem. Commun.*, 2011, **47**, 11128; (*j*) A. Mishra, J. Yano, Y. Pushkar, V. K. Yachandra, K. A. Abboud and G. Christou, *Chem. Commun.*, 2007, 1538; (*k*) E. Y. Tsui, R. Tran, J. Yano and T. Agapie, *Nat. Chem.*, 2013, **5**, 293; (*l*) C. Zhang, C. Chen, H. Dong, J.-R. Shen, H. Dau and J. Zhao, *Science*, 2015, **348**, 690; (*m*) A. A. Alaimo, D. Takahashi, L. Cunha-Silva, G. Christou and T. C. Stamatatos, *Inorg. Chem.*, 2015, **54**, 2137; (*n*) R. O. Fuller, G. A. Koutsantonis, I. Lozic, M. I. Ogden and B. W. Skelton, *Dalton Trans.*, 2015, **44**, 2132; (*o*) C. Chen, C. Zhang, H. Dong and J. Zhao, *Dalton Trans.*, 2015, **44**, 4431; (*p*) S. Mukherjee, J. A. Stull, J. Yano, T. C. Stamatatos, K. Pringouri, T. A. Stich, K. A. Abboud, R. D. Britt, V. K. Yachandra and G. Christou, *Proc. Natl. Acad. Sci. U. S. A.*, 2012, **109**, 2257; A. A. Alaimo, E. S. Koumousi, L. Cunha-Silva, L. J. McCormick, S. J. Teat, V. Psycharis, C. P. Raptopoulou, S. Mukherjee, C. Li, S. D. Gupta, A. Escuer, G. Christou and T. C. Stamatatos, *Inorg. Chem.*, 2017, **56**, 10760 (and refs therein); (*q*) A. Escuer, J. Mayans, M. Font-Bardia, M. Górecki and L. Di Bari, *Dalton Trans.*, 2017, **46**, 6514; (*r*) J. Mayans, M. Font-Bardia, L. Di Bari, M. Górecki and A. Escuer, *Chem. – Eur. J.*, 2018, **24**, 18705.

6 (*a*) C. Kozoni, E. Manolopoulou, M. Siczek, T. Lis, E. K. Brechin and C. J. Milios, *Dalton Trans.*, 2010, **39**, 7943; (*b*) C. Kozoni, M. Siczek, T. Lis, E. K. Brechin and C. J. Milios, *Dalton Trans.*, 2009, **42**, 9117.

7 M. Llunell, D. Casanova, J. Girera, P. Alemany and S. Alvarez, *SHAPE, version 2.0*, Barcelona, Spain, 2010.

8 D. Kuzek and R. J. Pace, *Biochim. Biophys. Acta*, 2001, **1503**, 123.

9 N. F. Chilton, R. P. Anderson, L. D. Turner, A. Soncini and K. S. Murray, *J. Comput. Chem.*, 2013, **34**, 1164.

10 See for example: (*a*) N. Berg, T. Rajeshkumar, S. M. Taylor, E. K. Brechin, G. Rajaraman and L. F. Jones, *Chem. – Eur. J.*, 2012, **18**, 5906, and refs therein; (*b*) K. Mitra, D. Mishra, S. Biswas, C. R. Lucas and B. Adhikary, *Polyhedron*, 2006, **25**, 1681; (*c*) J. B. Vincent, H. L. Tsai, A. G. Blackman, S. Wang, P. D. W. Boyd, K. Folting, J. C. Huffman, E. B. Lobkovsky, D. N. Hendrickson and G. Christou, *J. Am. Chem. Soc.*, 1993, **115**, 12353.